



Simple-jet mode electrosprays with water. Description, characterization and application in a single effect evaporation chamber

L.L.F. Agostinho^{a,b,*}, B. Bos^{a,b}, A. Kamau^b, S.P. Brouwer^{b,c}, E.C. Fuchs^b, J.C.M. Marijnissen^b

^a NHL Stenden University of Applied Sciences, Leeuwarden, The Netherlands

^b Wetsus European Centre of Excellence for Sustainable Water Technology, Leeuwarden 8900 CC, The Netherlands

^c Process and Energy Department, Energy Technology section, Delft University of Technology, The Netherlands

ARTICLE INFO

Keywords:

Electrohydrodynamic atomization
Simple-jet mode
Evaporation

ABSTRACT

Electrohydrodynamic atomization (EHDA) is a technique which uses the influence of strong electric fields to manipulate the break-up of a liquid, pumped through a capillary nozzle, into droplets. In this work, an extended description of a specific high flow EHDA mode, known as the simple-jet mode, is presented. In it, a review of different works published about the mode is presented as well as results about the droplet population generated with varicose and whipping break-up using water as the atomized liquid. Additionally, experiments were conducted to investigate whether such atomization method could be used to improve the efficiency of droplet in air evaporation, using a single effect evaporation chamber coupled with a EHDA multinozzle system functioning as a shower head. The liquid used in these experiments was a solution of water and NaCl (35 g L⁻¹) to simulate sea water average concentrations. The results have shown that, the manipulation of the droplet diameter, droplet size distribution and spray angle, provided by EHDA, could improve the droplet evaporation efficiency by up to 40% when combined with, e.g. forced convection and higher inlet temperatures.

1. Introduction

The disintegration of a liquid into droplets, also denominated atomization, can happen by various means. The mostly applied mechanisms are pressure (Maniarasan & Nicholas, 2009), ultrasonic oscillations and centrifugal forces (Siringano, 2010). Normally, these methods don't offer a fine control of the produced droplets' size, size distribution and/or the spatial dispersion (droplet-droplet distance). Regarding applications, pressure swirl atomizers are largely used in gas turbine combustors, rocket engines, diesel engines, and industrial burners (Liu et al., 2018). Ultrasonic atomization is commonly used for the production of fine (micro)droplets like those used in drug delivery systems (Briceño-Gutierrez, Salinas-Barrera, Vargas-Hernández, Gaete-Garretón, & Zanelli-Iglesias, 2015). For large flow systems, such as thermal desalination, wind break and pneumatic atomizers are commonly used (Ashgriz, 2011). In many applications, e.g. evaporation, spray drying, painting systems, it is known that well (spatially) dispersed droplets with specific size and narrow size distribution are desirable (Williams, 1958). A process which can achieve this requirement is electrohydrodynamic atomization (EHDA), also known as electrospray.

EHDA produces charged droplets formed from the break-up of a liquid in the presence of a strong electric field (kV·cm⁻¹) (Grace

* Corresponding author at: NHL Stenden University of Applied Sciences, Leeuwarden, The Netherlands.

E-mail addresses: luewtonlemos@gmail.com, luewton.agostinho@hvhl.nl (L.L.F. Agostinho).

<https://doi.org/10.1016/j.jaerosci.2018.04.010>

Received 31 October 2017; Received in revised form 30 April 2018; Accepted 30 April 2018

Available online 05 May 2018

0021-8502/ © 2018 Elsevier Ltd. All rights reserved.

& Marijnissen, 1994). To create the desirable electric field different setups can be used comprising a (capillary) nozzle placed close to a counter electrode, which can be a metallic plate or a ring, positioned below the nozzle tip (nozzle to plate or nozzle to ring down configuration) or above it (nozzle to ring up configuration). The configuration to be used basically depends on the desired application, meaning: applications which require droplets (material) deposition on a substrate normally use the nozzle to plate configuration (Jaworek et al., 2016) while applications which require a longer stay of the droplets in the air, such as bipolar coagulation (Borra, Camelot, Marijnissen, & Scarlett, 1997; Camelot, Marijnissen, & Scarlett, 1999) and greenhouse applications (Geerse, Marijnissen, Kerssies, van der Staaij, & Scarlett, 1999) normally use the nozzle to ring (up or down) configuration. Two good reviews about the process are also presented in this special edition (Ganan-Calvo, Lopez-Herrera, Herrada, Ramos, & Montanero, 2018; Rosell-Llompart, Grifoll, & Loscertales, 2018).

When operated in the so called “cone-jet mode” (Cloupeau & Prunet-Foch, 1989; Gañan-Calvo & Barrero, 1996; Gañan-Calvo & et al., 2009; Hartman, Brunner, Camelot, Marijnissen, & Scarlett, 1999; Hartman, Marijnissen, & Scarlett, 1997; Tang & Gomez, 1995) the process offers a fine control of the generated droplets size (much smaller than the nozzle inner diameter) and can produce very narrow droplet size distributions, i.e. monodispersed sprays (Gañan-Calvo, 1997). In this case, it is mostly used in applications which require narrowly distributed nanometer to micrometer-size droplets like mass spectrometry (Juraschek & Röllgen, 1998; Tang, Page, Kelly, & Marginean, 2017), production of thin films (Jaworek et al., 2016) and drug delivery (Ciach, 2007; Geerse & Marijnissen, 2003; Loscertales et al., 2002; Nguyen, Clasen, & Van den Mooter, 2016), powder production and surface coating (Jaworek, Krupa, & Sobczyk, 2018), electrodes coating (Castillo, Martin, Rodriguez-Perez, Higuera, & Garcia-Ybarra, 2018; Kelder, Marijnissen, & Waiyego, 2018) and biomedical applications (Boda, Li, & Xie, 2018). In this review, Llompart et al give an overview about EHDA in this mode (Rosell-Llompart et al., 2018).

A known drawback of EHDA in this mode is its limitation when the liquid to be atomized is water (Borra, Ehouarn, & Boulaud, 2004; Borra, 2018; Stachewicz, Dijkman, Burdinski, Yurteri, & Marijnissen, 2009). In this case the challenge lies basically on the high surface tension of water which imposes the application of a very strong electric field to allow a stable atomization and, in most cases, the limit for sparking is reached before the needed field intensity is established. A good overview about electro spraying water in the cone-jet mode is given by Stachewicz et al. (2009). In their work, the authors have mentioned the different challenges that other authors faced when spraying water in this mode. Additionally, they have shown a possible way to spray the liquid in a “stable pulsed cone-jet mode” using short time voltage pulses. Another possible way to overcome this issue was presented by Parmentier et al. (2016). In their work the authors used concentric nozzles with water as the inner liquid and (different) ionic liquids as the outer liquid, to spray in the cone-jet mode and used electrophoretic forces to enhance the migration of metallic ions from the water phase into the ionic liquid phase. In this case, water is not used as the (main) atomized liquid, but it can be encapsulated in other liquids while sprayed in the cone-jet mode. Such technique allows the formation of very small (encapsulated) water droplets. Lastly, Kamau, Agostinho, Gatari, and Marijnissen (2017) and Bos (2017) also presented a rather simple solution to allow atomization of water in the cone-jet mode by using a second liquid as surrounding medium, i.e. instead of air, and managed to electro spray water in a continuous and stable cone-jet mode in ethylene-glycol and hexadecane. In this edition, a review about the same topic is presented by Borra (Borra, 2018).

Another (known) drawback of EHDA in the cone-jet mode is the fact that it operates at very low flow rates (μL - mL per hour per nozzle). Focusing on this problem, some authors have proposed electrohydrodynamic atomization in another mode, i.e. the simple-jet mode, as an option for systems which require a high throughput and monodispersed charged droplets in the (sub)millimeter range (Agostinho, 2013; Ondimu O.M, 2017). The first author who has mentioned about such (high flow) mode was probably Taylor (Taylor, 1969). Even though in his work the author did not (specifically) talk about electrohydrodynamic atomization, he did present the behavior of an (water) electrified jet using flow rates compatible with the simple-jet mode. After him Balachandran, Machowski, and Ahmad (1992) reported the effect of strong electric fields in high-flow (1.9 mLmin^{-1}) electrostatic atomization and called what they have seen the “smooth jet mode”. The characteristics of electro spray with high and low flows were, later on, described by both Grace and Marijnissen (1994) and Cloupeau and Prunet-Foch (1994). Only then, the term “simple-jet” was used to denominate the mode.

Experimentally it has been also shown that the simple-jet mode offers control of the spray angle, making it a very good option for, e.g. evaporation-distillation processes (Agostinho, Yurteri, Fuchs, & Tamminga, 2012) and/or greenhouse applications (Geerse et al., 1999). Aiming at even higher throughputs, Agostinho et al. (2013) have reported a novel multi nozzle design which allowed atomization in the Lh^{-1} range with five nozzles. The proposed design was able to produce droplets with the same average size for all nozzles and allowed a continuous and stable operation of the spray inside chambers with up to 95% relative humidity level.

When compared to the cone-jet mode, electro spraying water in the simple-jet mode is considerably less challenging, as it does not require the fine balance of forces required by the former one.

In this paper the authors will present a description of EHDA in the simple-jet mode specially focused on water as the liquid to be atomized. Additionally, as an application example, an experimental part is presented in which a EHDA multinozzle system, operating in the same mode, is coupled to a single effect evaporation chamber to evaluate whether the manipulation of the droplet size and spray angle (droplet to droplet distance) provided by electro spray can be used to influence the overall efficiency of the system.

2. Electro spray in the simple-jet mode

Only few authors have published about the simple-jet mode. According to Cloupeau and Prunet-Foch (1990) it appears when, in the presence of an (strong) electric field, the flow rate through the nozzle is sufficiently high to form a permanent jet on its output. Moreover, they also mentioned that this mode can be obtained for flow rates lower than the critical (jetting) rate, if the electric field

intensity is increased sufficiently to create a jet.

Grace and Marijnissen (1994) mentioned the following: “The simple-jet and the cone-jet exhibit similar structures. The transition between the two is sharp for high conductivity liquids and vague for low conductivity liquids. Both consist of a single jet drawn from the meniscus by electrical forces.”. Moreover they said that: “The simple-jet differs from the cone-jet in the sharpness of the conical meniscus and in this mode break-up usually occurs via varicose instabilities”. Lastly, in the electrospray mode diagram presented by these authors, the simple-jet mode is positioned on the right side of the cone-jet mode, i.e. at same potential level but at higher flow rates. Clearly the authors have observed the differences between the modes but were unable to give accurate details due to the limitations of the observation tools available to them. Balachandran et al. (1992) performed experiments using flows of some mL min^{-1} (from the figures published in their work, clearly inside the simple-jet mode range) and indicated that, the use of AC frequencies, superimposed on DC fields, could decrease the whipping of the jet. Agostinho, Yurteri, Fuchs, and Tamminga (2010) are probably the only authors (so far) to dedicated a complete work to the simple-jet mode. In their work, the authors presented an extensive description of the spray for different solutions, i.e. deionized water and salt water, and reported the influence of the flow rate and electric potential for a constant nozzle to ring distance on the droplet size, spray angle, jet break-up length and droplet size distribution.

Even though (most of) the currently available scientific literature dedicated to classify the electrospray modes define the simple-jet mode as a “high flow” mode and the cone-jet a “low flow” mode, a more quantitative approach to define the flow rate limits between these two modes is possible. For that, the studies done in fluid dynamics to define the different droplet formation mechanisms, also known as droplet formation “regimes”, of inviscid, capillary, uncharged liquid jets, can be used (Ambravaneswaran, Phillips, & Basaran, 2000; Clanet & Lasheras, 1999; Eggers & Villermaux, 2008; Hoeve et al., 2010; Rayleigh, 1879). These works mention that, when a liquid is slowly pumped through a (capillary) nozzle, it forms a pendant droplet, which grows in a quasi-static balance between gravitational and surface tension forces before it finally detaches from the liquid meniscus. According to them, the droplet formation mechanism in this case is known as the “dripping regime”. If the flow rate is further increased, eventually a continuous jet will be formed at the nozzle tip, which breaks-up due to Plateau-Rayleigh instabilities, finally generating the droplets at the tip of the broken jet. If such conditions are reached, it is then said that the droplets are being formed in the “jetting regime” (Ambravaneswaran et al., 2000; Clanet & Lasheras, 1999; Eggers & Villermaux, 2008; Lafrance, 1975). A very specific formation mechanism happens between the dripping and the jetting regime. In this case, the droplets are not detaching directly from the nozzle tip, and also not from a liquid jet; rather, they are breaking-up from a small, unstable, liquid ligament, formed at the nozzle tip. This formation mechanism is denominated “dripping faucet” or “transition regime”. A more illustrative representation of these three droplet formation mechanisms, i.e. from now on denominated “regimes”, for uncharged jets, is depicted in Fig. 1.

Quantitatively, the transition between these regimes depends basically on the kinetic energy of the liquid, which can be defined as a function of the nozzle geometry, the applied flow rate and the liquid density and surface tension. Van Hoeve et al. (2010) mentioned that, the lower critical velocity for jet formation, in capillary flows, can be expressed in terms of the liquid Weber number (We) as presented below,

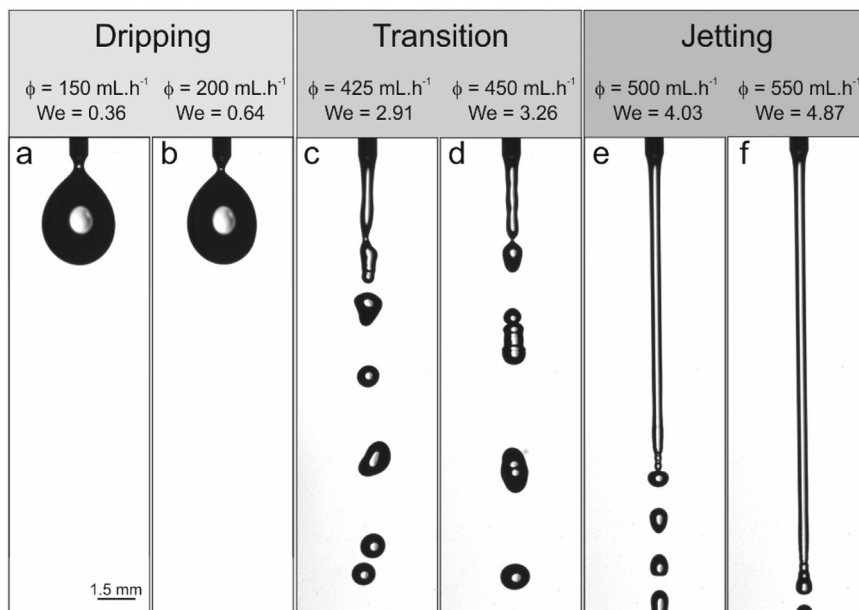


Fig. 1. Different droplet formation mechanisms, or formation “regimes”, for uncharged, inviscid, capillary liquids, pumped through a capillary nozzle. Droplet formation mechanism in the “dripping regime” (1a and 1b), droplet formation mechanism in the “transition regime” (1c and 1d) and droplet formation mechanism in the “jetting regime” (1e and 1f). The respective flow rate (ϕ) and Weber number (see Eq. 1) are presented above for each figure.

$$We = \frac{\rho_l r v^2}{\gamma} > 4, \quad (1)$$

where ρ_l is the liquid density, r is the jet radius (normally related to the nozzle inner radius), v is the liquid velocity and γ is the liquid surface tension, respectively.

Agostinho (2013) performed different experiments with uncharged jets using deionized water and deionized water with NaCl solutions ($35 \text{ g}\cdot\text{L}^{-1}$) as the atomized liquid, with different capillary nozzles, and found that, within the experimented conditions, the dripping regime occurs at $We < 2.5$, the transition occurs at $2.5 \leq We \leq 4$; and at $We > 4$ the jetting regime takes place.

If the relative velocity between the jet and the surrounding air can no longer be neglected, aerodynamics effects change the break-up and another droplet formation regime takes place, the wind-induced regime. This regime is not within the scope of this work, thus it will not be further explored.

These droplet formation regimes for uncharged jets have been extensively studied. The above presented limits thus are only a small part of a large amount of information known about the process and represent a specifically chosen window for the contents of this paper. Other studies also relate different jet diameters and other dimensionless numbers, e.g. the Reynolds number, Ohnesorge number, and liquid velocity, to these regimes (Eggers & Villermaux, 2008). A diagram showing the different regime limits for water with different nozzle diameters, including the wind-induced regime, has also been presented by Hoeve et al. (2010).

When such classification is implemented in electrohydrodynamic atomization, i.e. charged jets, one can say that modes like the cone-jet mode and the intermittent cone-jet mode are dripping regime modes and the simple-jet mode is, therefore, a jetting regime mode. Taking this into account, one could add that the simple-jet mode takes place whenever a strong electric field is applied to liquid atomization with Weber number bigger than 4. Additionally, as also mentioned by Cloupeau and Prunet-Foch (1994), it is also possible to force the formation of the simple-jet mode inside the transition regime ($We < 4$), by increasing the electric field intensity.

The diagram below (Fig. 2) describes the relation between the liquid flow rate and the electric potential on the formation of the different EHDA modes with a clear quantitative reference to the different droplet formation regimes.

The diagram shows that the simple-jet mode can be formed inside the transition regime and the jetting regime, for a broad range of electric fields. Once inside the simple-jet mode, changing the electric field magnitude will create different droplet break-up mechanisms, namely: varicose, whipping or ramified break-up.

For lower intensities of the applied electric field, the formation of the droplets happens due to Rayleigh-Plateau instabilities, i.e. varicose break-up. In this region, it is difficult to see differences between the break-up mechanism in this situation and what is seen for uncharged jets. However, the implementation of the electrical stresses in this case decreases the jet radius, which causes a consequent decrease of the fastest growing wavelength and a decrease of the primary droplet size (Collins, Harris, & Basaran, 2007; Zeleny, 1917).

If the electric field intensity is further increased the break-up mechanism changes from varicose to whipping break-up. In this case the influence of the strong(er) electric field on the liquid surface causes off-axis instabilities which grow forcing the jet to whip during break-up. Some authors have reported about this break-up mechanism for EHDA with low flows (Camelot, Brunner, Hartman, Marijnissen, & Scarlett, 1998; Hartman, Brunner, Camelot, Marijnissen, & Scarlett, 2000) and high flows (Eggers & Villermaux, 2008; Hohman, Shin, Rutledge, & Brenner, 2001a, 2001b; Taylor, 1969). Among them, it is important to mention the work done by Camelot (D. M. A. Camelot et al., 1998) and Hartman (Hartman et al., 2000), who reported that, in order to create this kind of stability, the ratio between the surface tension stresses and the electric stresses on the jet surface has to be bigger than 0.3.

If the electric field intensity is increased even further, the electric stresses overcome the liquid surface tension causing the

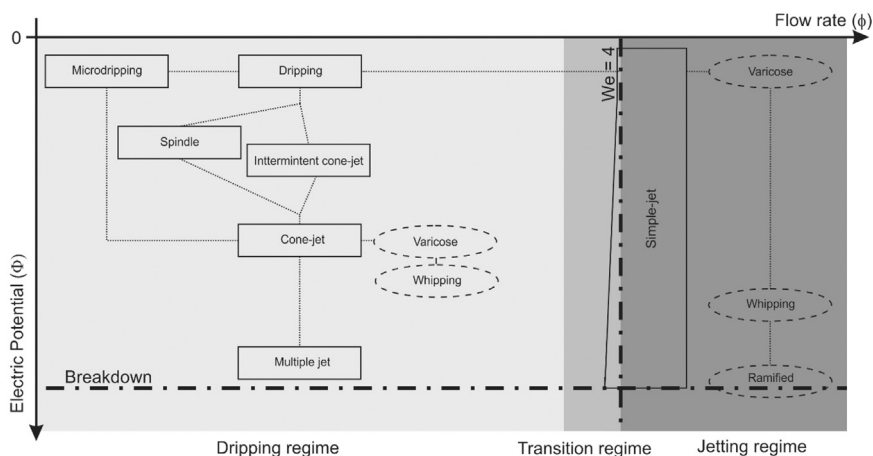


Fig. 2. Diagram adapted from Agostinho (2013) representing the different EHDA modes within the different atomization regimes and their relation to flow rate and electric potential for a constant nozzle to counter electrode distance. The small rectangles represent the different EHDA modes while the (dashed) ellipsoids represent the break-up mechanisms for a specific EHDA mode. The dashed-dotted lines represent the breakdown limit (horizontal) and the jetting regime ($We = 4$) limit (vertical line).

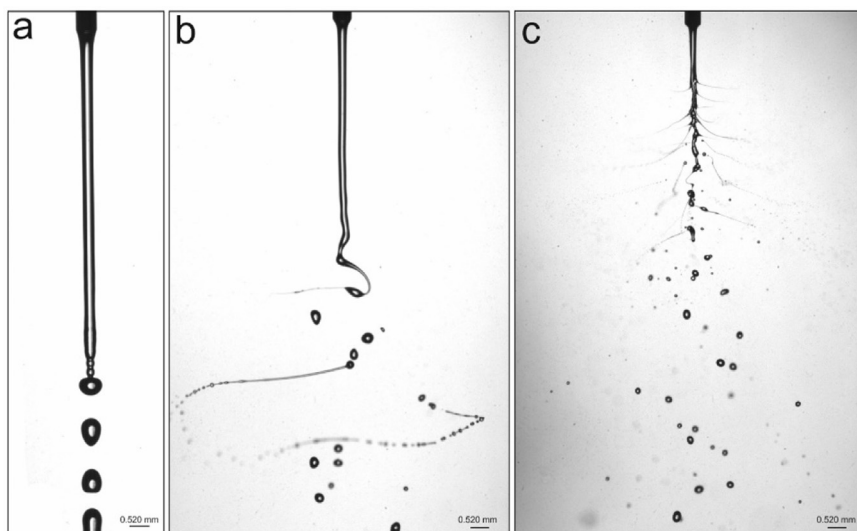


Fig. 3. Three examples of break-up mechanisms in the simple-jet mode: varicose break-up (3a), whipping break-up (3b) and ramified break-up (3c). Fig. 3a and b are snap shots done with deionized water, using $300 \text{ mL} \cdot \text{h}^{-1}$ flow rate, at 9 kV (Fig. 3a) and 18,5 kV (Fig. 3b). Fig. 3c was done with ethanol (99%), using $300 \text{ mL} \cdot \text{h}^{-1}$ flow-rate and 18.9 kV. In all pictures the setup used was nozzle to ring (up) configuration with the same nozzle (OD = 0.52 mm and ID = 0.25 mm) and same nozzle to ring distance (2 cm). The ring (outer) diameter in this case was 5.4 cm.

formation of “secondary” jets, from where new (electro)sprays will be formed along the extension of the main jet. This is called “ramified break-up”. These three different break-up mechanisms, for the simple-jet mode, are shown in Fig. 3.

Agostinho, Yurteri, Fuchs, Marijnissen et al. (2012) studied the droplet size and size distribution for the simple-jet mode with varicose break-up for different nozzle sizes and a broad range of electric field intensities. As expected, in this case, the droplet size can be determined using the relation proposed by Rayleigh for uncharged jets, i.e. $D_d \cong 1,8 D_{\text{jet}}$ which leads to a direct conclusion that, in this mode, the droplet diameter is relatively dependent on the jet diameter, thus, on the nozzle inner diameter. If the electric field is increased sufficiently, the electric stresses will cause the constriction of the jet which will lead to a consequent decrease of the average droplet size. In their work, the authors found reductions of the primary droplet average diameter up to 20%, when compared to uncharged situations, for the jetting regime ($We > 4$), and up to 50% in the transition regime ($We < 4$).

Other important results presented in the same work were: (i) the application of the electric field produced a narrower size distribution, leading to, in some cases, the formation of monodispersed sprays ($RSD < 0.20$), (ii) the spray angle can be manipulated via the electric potential for the same flow rate and nozzle to ring distance, i.e. higher electric potentials produce bigger spray angles, (iii) higher potentials, for the same flow rate and nozzle to ring distance, lead to shorter jet break-up lengths and (iv) the droplets generated in this mode carry a charge between 5% and 20% of their Rayleigh limit.

In another work the same authors also investigated the influences of the liquid electric conductivity on the performance of the spray (Agostinho, Yurteri, Fuchs, & Tamminga, 2012). For that they conducted experiments with deionized water and salt water with different concentrations (from 17 to $70 \text{ g} \cdot \text{L}^{-1}$). The authors concluded that, within the tested range, the electrical conductivity of the liquid did not significantly change the limits where the jet starts to whip and the spray angle, i.e. droplet to droplet distance. The authors also investigated influences on the diameter of the primary and satellite droplets and found that, for the primary droplets, there is no significant change caused by the changes in electric conductivity. However, in the case of satellite droplets, an inverse correlation was found, i.e. higher conductivity water electrospays ($35 \text{ g} \cdot \text{L}^{-1}$) produced satellite droplets up to 20% bigger when compared to the same conditions using deionized water. These results are rather important for a good understanding of the second part of this paper, when the performance of a single step evaporator is tested for electrospays operating in the simple-jet mode using solutions with the same salt concentrations.

Not much is known so far about the characteristics of the droplet population generated in the simple-jet mode with whipping break-up. Due to this fact, some experiments were performed by the authors to provide a bit more insight about this population. The results are presented in Fig. 4.

The experiments conducted to generate the above presented data were performed with deionized water, a nozzle to ring (up) setup, nozzle ID = 0.41 mm (OD = 0.72 mm) and nozzle to ring distance equal to 2 cm (outer diameter of the ring equal to 5.4 cm). The tests were performed with a constant flow rate of $500 \text{ mL} \cdot \text{h}^{-1}$ ($We = 4.03$ uncharged situation), while the electric potential (applied on the ring with grounded nozzle) was varied from 13.3 kV (still varicose) to 19 kV (whipping).

From the data it is possible to infer that the droplet population generated in the simple-jet mode with whipping break-up is rather polydispersed. As observed in Fig. 4a, for 13.3 kV the break-up is still varicose. This low potential was (also) investigated to provide a direct comparison between the droplet population generated in the varicose and the whipping break-up. In the former break-up type a quite narrow size dispersion with primary droplet average diameter around twice the jet diameter and some (low density) populations of satellite droplets is generated (Fig. 4g). As soon as the whipping break-up starts, a polydispersed droplet population

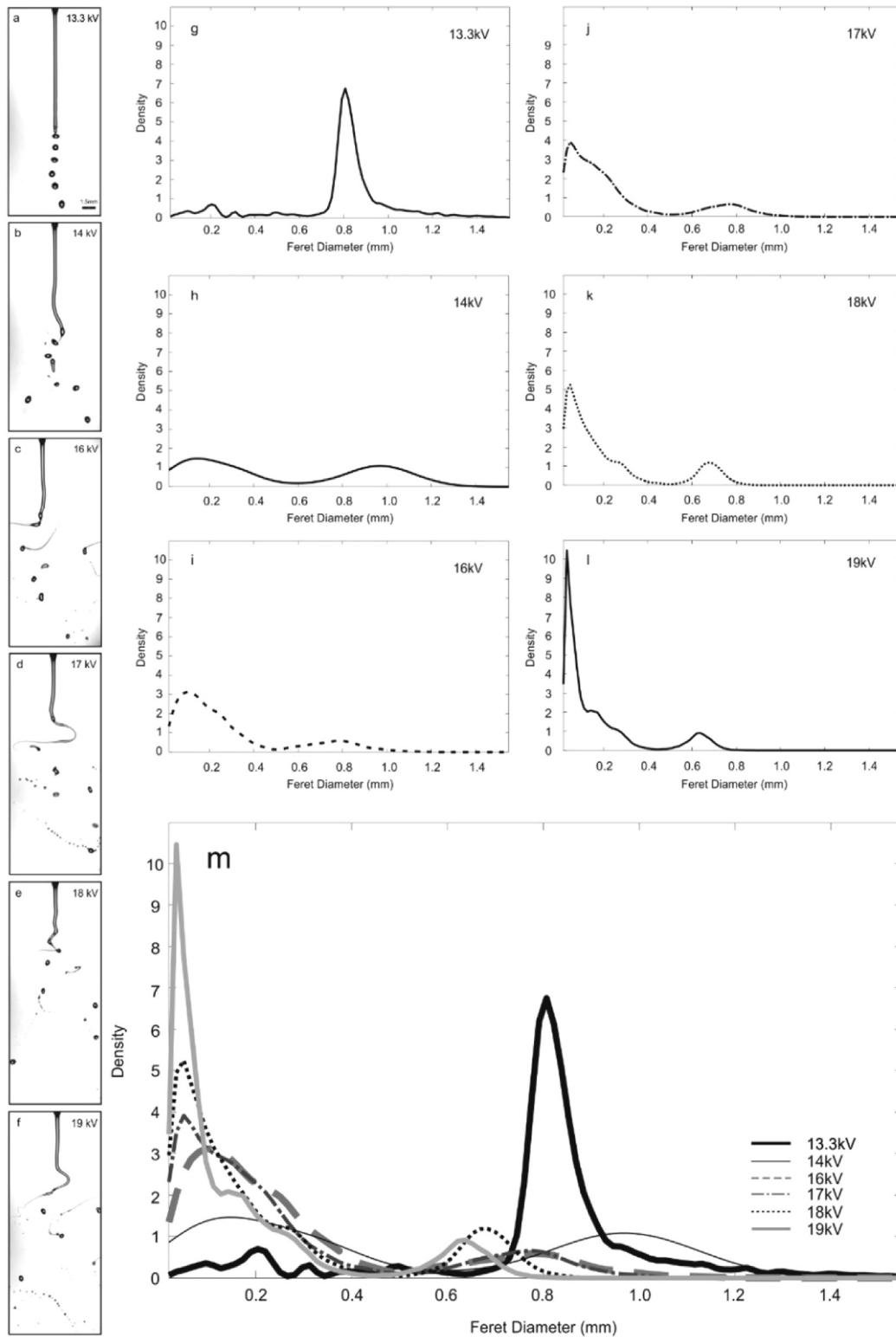


Fig. 4. High speed imaging snapshots of the simple-jet mode with varicose (4a) and whipping break-up at different electric potentials (4b - 4f) and analysis of the generated populations in each case represented as probability density function plot (4g - 4l). A combined plot with the different probability density plots obtained in each situation is presented in Fig. 4m. All tests were performed using deionized water and a nozzle to ring (up) configuration, with nozzle ID = 0.41 mm and OD = 0.72 mm, flow-rate (500 mL h^{-1}), nozzle to ring distance (2 cm) and ring outer diameter of 5.4 cm.

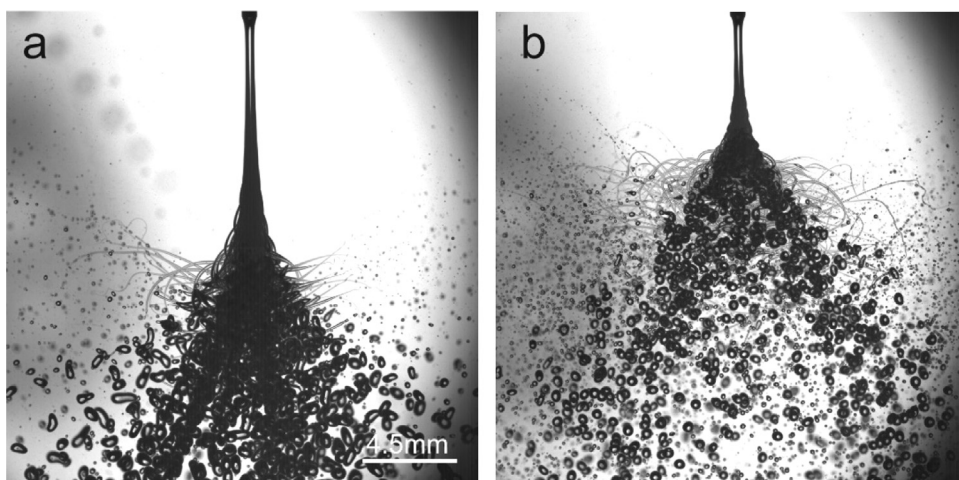


Fig. 5. Superposition of 100 images from recorded high speed movies of different electrospays in the simple-jet mode with whipping break-up. Both stacks were created with deionized water electrospays, 500 mL h^{-1} flow rate, nozzle OD = 0.72 mm and ID = 0.41 mm, and a nozzle to ring (up) configuration with the ring placed at 2 cm from the nozzle tip and ring outer diameter 5.4 cm. The electric potentials were 14 kV (Fig. 5a) and 19 kV (Fig. 5b).

appears. In the case of 14 kV the populations can be basically considered as a “big droplets and small droplets population” (two distinct, rather normally distributed populations). The average diameter of the “big droplets” population is slightly bigger than the average size of the primary droplets obtained with 13.3 kV in the varicose break-up, i.e. $\sim 0.9 \text{ mm}$, and the “small droplets” average diameter is at around $150 \mu\text{m}$.

If the electric potential is further increased there are clear trends, namely: (i) the main peaks (big droplets and small droplets) for all the populations shift to the left, i.e. the big and the small droplets population’s average diameter decreases, and (ii) the big droplets population frequency decreases while the small droplet population frequency increases.

To provide a visual reference for these trends, two different image stacks (superposition of approximately 110 images) were created for 14 kV and 19 kV (see Fig. 5). For comparison reasons the stacks were produced with the same number of images and the same frame rate (12.500 fps), giving an indication of the droplet production rate (droplets per second) in both cases. As can easily be seen in Fig. 5, within the whipping mode a (negative) correlation between applied potentials and droplet size (big and small droplets population) occurs.

A representation of the impact caused by the different electric potentials on droplet density is presented in Fig. 6. The figure displays the cumulative density plots of the droplet populations generated in all the break-up situations displayed on Fig. 4. From there it is possible to see that, from the varicose break-up potential (13.3 kV) up to the highest whipping break-up potential (19 kV), the D_{50} decreases from $\sim 820 \mu\text{m}$ at 13.3 kV to $\sim 90 \mu\text{m}$ at 19 kV. At the same time, the D_{80} decreases from $\sim 900 \mu\text{m}$ at 13.3 kV to $\sim 250 \mu\text{m}$ at 19 kV. This data indicates that the simple-jet mode with whipping break-up can be used to create relatively big populations of droplets smaller than the nozzle inner diameter with high flow rates.

Moreover, it is important to mention that, the tool used to characterize the droplet diameter in this case was an optical one (high speed imaging) with a lower detection limit of $\sim 15 \mu\text{m}$.

Extra experiments were performed following the same method for a different nozzle diameter (OD = 0.52 mm and ID = 0.25 mm) and different flow rates, i.e. 300 mL h^{-1} , 400 mL h^{-1} and 600 mL h^{-1} and the obtained results followed the same trend.

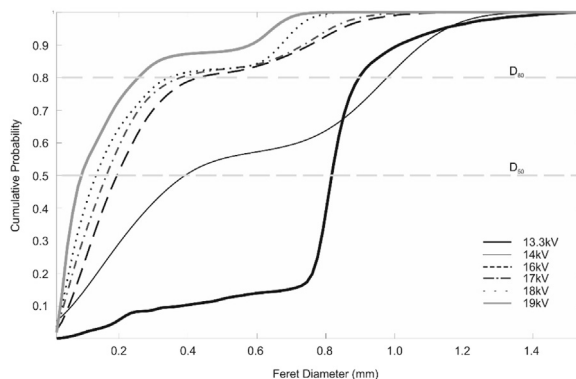


Fig. 6. Cumulative density plots of droplet populations generated in all the different break-up situations of Fig. 4, i.e. from potentials 13.3 till 19 kV. The lower dashed (grey) line represents D_{50} and the upper dashed (grey) line represents D_{80} .

More recently, other publications have covered specific aspects of the simple-jet mode. An example is the work of Ondimu et al. (2017), in which a 2D model was derived to describe the trajectories of the electrospayed droplets. In the same article, the authors reported a shift between the droplet mass and charge center shortly after the break-up, which is claimed to be a very plausible explanation for the initial dispersion of the droplets. Gachara, Bos, Marijnissen, Gatari, and Agostinho (2017) reported the atomization of non-Newtonian solutions with high solid content. Lastly, Park, Hong, Kim, and Kim (2017) recently reported some experiments with water in the same mode.

3. Experimental method. Applying the simple-jet mode in a single step evaporation system

A few characteristics of the sprays are especially important in spray evaporation processes. These are, amongst others, the droplet size, the inter-droplet distance (also referred as droplet packing density) and the size distribution. The correlation between these characteristics and the evaporation efficiency has been explored in the past, both for fuel and for water droplets (Li, Nishida, & Hiroyasu, 2011; Sinha, Surya Prakash, Madan Mohan, & Ravikrishna, 2016; Wang, Xu, Song, & Jiang, 2017). However, most of the are either theoretically conducted or did not offer the possibility of changing all the parameters as it is possible with EHDA systems.

Taking this into consideration, some experiments were conducted to evaluate whether the relatively easy manipulation of the droplet size, size distribution and spray angle, provided by electrospay in the simple-jet mode, could be used to influence the evaporation efficiency of droplets electrospayed in a single step evaporation chamber. Such systems are frequently used in different

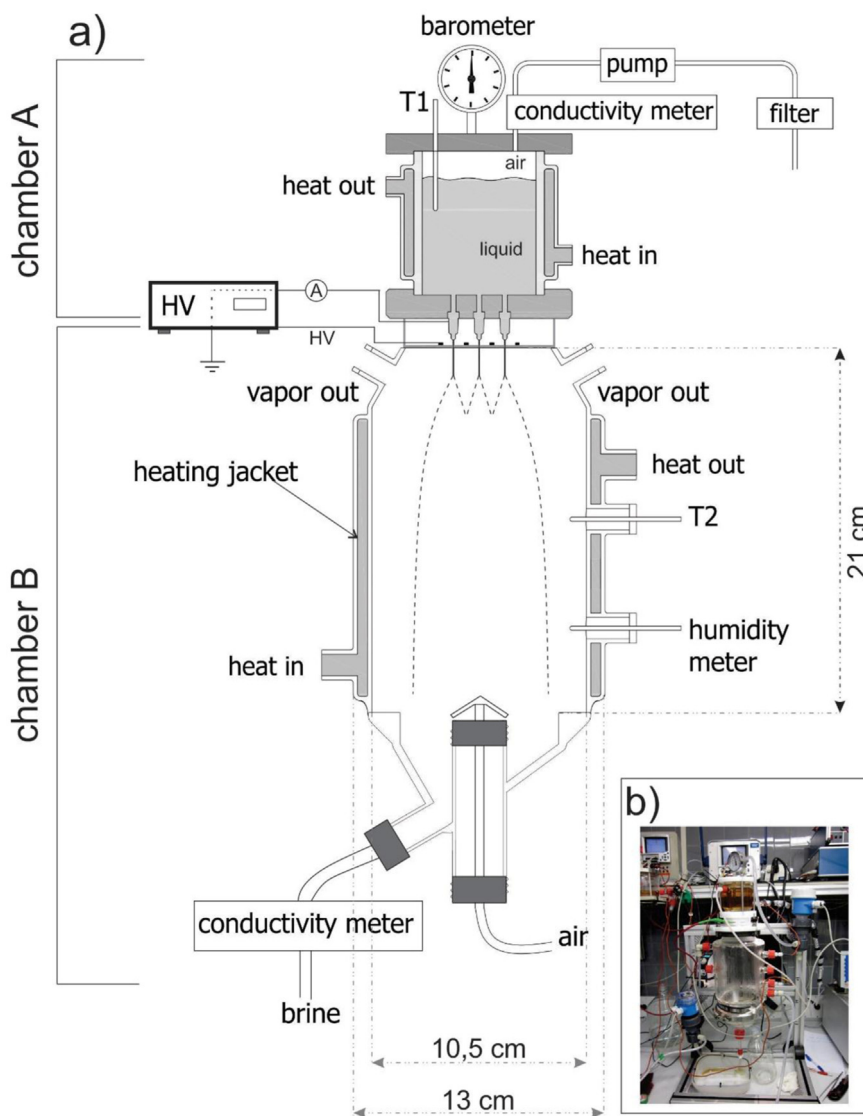


Fig. 7. (a and b). Fig. 7a is a technical drawing of the multi-nozzle EHD atomizer coupled with single-effect evaporator (chamber A and B). Fig. 7b is a photograph of the real setup.

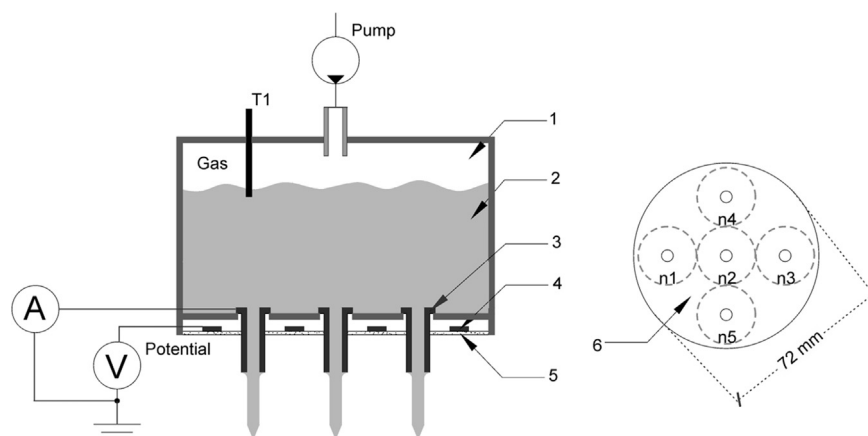


Fig. 8. Schematic diagram of chamber A consisting of a gas column (1), salt solution (2), nozzles (3), copper rings (4), insulation layer (5). The nozzles and rings are organized in a circular pattern (6) (Figure from Brouwer (2011)).

industrial processes, e.g. spray drying systems and thermal desalination. In the experiments, the atomized solution chosen was a solution of deionized water and NaCl (35 g L^{-1}), i.e. average seawater salt concentration.

Fig. 7 is a representation of the experimental setup. It is a combination of an evaporation chamber, denominated “chamber B”, and a top head EHDA multi-nozzle setup with pre-heating, denominated “chamber A”.

The multinozzle device and pre-heating chamber are the same as previously reported by Agostinho et al. (2013). It was composed of 4 nozzles placed around a central one in a 36 mm radius circle which gives a packing density of $2 \cdot 10^3$ nozzles per m^2 (Fig. 8). The counter electrodes were interconnected copper rings positioned at 1.7 cm above the nozzle tip with 2 cm diameter. High voltage (FUG HCP 14–20000 DC) was applied to the rings while the liquid and nozzles were grounded. The nozzles were blunt ended, polished, stainless steel needles (FED Inc.) gauge number 22, 250 μm ID and 510 μm OD, uncoated. An insulating layer (circuit board FR-4) was placed between the rings and the nozzles to electrically isolate them from the rest of the device. To assure an uniform liquid flow through the nozzles and to decrease possible oscillations from the pump, an air gap was kept above the liquid/air interface inside the pre-heating chamber which gets pressurized (1.2–1.6 bar absolute pressure) due to the action of the pump. The liquid was pumped (SIMDOS® FEM 1.10 KT.18S model) from a tank and filtered with a carbon filter (BOSCH F4058) to prevent blockage of the nozzles. Temperature probes (PT100), indicated in Figs. 7 and 8 as T_1 , were used to continuously measure the inlet temperature.

Chamber B (Fig. 7) was made of borosilicate glass to allow the visualization of the spray. A PT100 temperature probe (shown in Fig. 6 as T_2) was used to measure the temperature inside the chamber and a humidity meter was used to measure the relative humidity. A heating jacket provided a constant temperature of the evaporation chamber wall (chamber B) throughout the experiments (25°C). Dry (ambient temperature) air was introduced from below, counter-currently with the spray, using a T-shaped air diffuser to provide forced convection and its flow rate could be adjusted and was measured with a flow meter (KOBOLD KFR-2218NO). The temperature of the injected dry air could not be monitored. However, prior to each experiment, a stabilization period was conducted to allow reaching steady state condition before starting the spray. In all cases the thermal jacket was able to provide the necessary heat flux so the temperature inside the chamber could be stable at around 25°C . Additionally, the humidity probe was used to verify whether the air flow rate was enough to keep humidity level inside the chamber below the saturation level. This was the case for all experiments. The electrical conductivities and temperatures of the influent and effluent (from now on referred as brine) were measured using a SMARTEC–T CLD 633 conductivity meter. All sensors mentioned were connected to a data logger (ENDRESS-HAUSSER RSG30). In all experiments, the condensate was blown out and the brine was collected.

Some physical-chemical properties of the used solution as well as of deionized water (for comparison) are shown in Table 1.

In all experiments the liquid was pre-heated before electro-spraying. Four different flow rates were used 240, 300, 360 and 420 $\text{mL h}^{-1}\text{nozzle}^{-1}$, which correspond to the Weber numbers, 3.2, 5.01, 7.22, and 9.81 respectively (uncharged conditions). Thus, three of the chosen flow rates were inside the jetting regime (300, 360 and 420 $\text{mL h}^{-1}\text{nozzle}^{-1}$) and one flow inside the transition regime (240 $\text{mL h}^{-1}\text{nozzle}^{-1}$) to also allow a comparison between the different regimes.

For each flow the electric potential was varied between 0 and 4 kV. These potentials are lower than those used in the first part of the paper due to the following reasons: (i) the evaporation experiments were conducted only with varicose break-up because the

Table 1

Physical properties of the deionized water and NaCl solution ($35 \text{ g} \cdot \text{L}^{-1}$) and deionized water. Measurements were conducted at ambient lab temperature.

Liquid	μ [$\text{Ns} \cdot \text{m}^{-2}$]	ρ [$\text{kg} \cdot \text{m}^{-3}$]	ϵ_r	K [$\text{S} \cdot \text{m}^{-1}$]	γ [$\text{N} \cdot \text{m}^{-1}$]
Dwater	1.00×10^{-3}	1.00×10^3	8.01×10^1	1.20×10^{-3}	7.19×10^{-2}
NaCl aq.	9.21×10^{-4}	1.05×10^3	7.35×10^1	4.5×10^0	7.3×10^{-2}

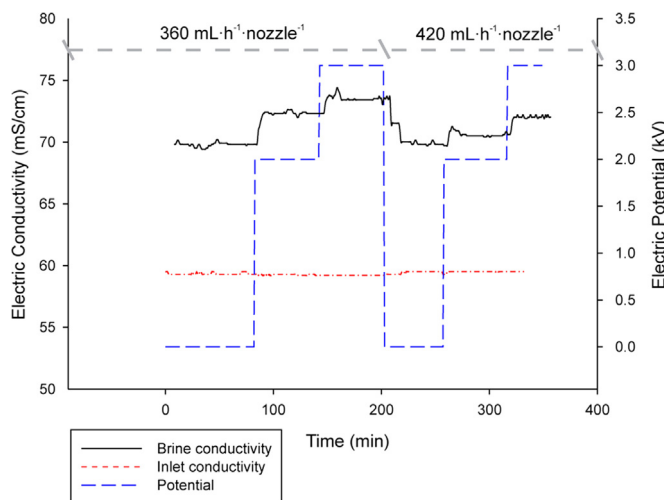


Fig. 9. Brine conductivity (solid line) and inlet conductivity (dot dashed line) for different potentials (dashed line) and two different liquid flow rates (360 and 420 mL·h⁻¹). Liquid pre-heated to 80°C.

whipping break-up provided a rather wide distribution of the droplets and would have required a larger chamber diameter to avoid contact between the droplets and the chamber wall, (ii) the nozzle to ring distance, and the nozzle diameter, in these experiments, were smaller to allow a more compact system for the reactor top head (chamber A).

For each combination of flow rate and electric potential, the evaporation was measured using a general mass balance, assuming steady-state conditions;

$$\% \text{evaporated} = \frac{(m_i - m_b)}{m_i} \times 100\% \quad (2)$$

where m_i is the inflow mass flow rate (kg h⁻¹) and m_b is the mass flow rate of the brine (kg·h⁻¹).

The influence of forced convection on evaporation was studied injecting dry air at ambient temperature at different flow rates (35, 45, 75 and 85 L min⁻¹). These experiments were conducted for 360 mL h⁻¹·nozzle⁻¹ (best performance flow-rate found in the first experiments) using different voltages (0–4 kV). The same conditions were used to verify the influence of the spray's initial temperature as well by pre-heating the inlet to different temperatures (60 and 80 °C).

The spray electric current was measured continuously in all experiments with an electrometer (Fluke 8846A 6.5) connected to the ground line to verify the stability of the spraying system during the experiments. All experiments were done in duplicate.

4. Results and discussion

Fig. 9 is a representation of initial experiments done to verify the effect of different applied potentials, i.e. in this case 0, 2 and 3 kV, on the brine conductivity. These experiments were also conducted to find out how stable the electrospray would perform in high humidity conditions and for long periods, i.e. every liquid flow rate vs electric potential configuration was operated for approximately one hour. The experiments were conducted with two liquid flow rates (360 and 420 mL h⁻¹ nozzle⁻¹) and the applied potential for each flow was programmed to shift automatically. The observed increase of the brine's electrical conductivity at higher electrical potentials with constant conductivity at the inlet is an indication of higher spray evaporation. Additionally a constant value of the brine conductivity at a certain electric potential is an indication that the spray was stable, which was also confirmed by constant values of the electric current recorded during the spray performance (not shown on the plot).

Another immediate inference taken from this first experiments is the negative correlation between the tested flows and the spray evaporation, i.e. higher flows lead to less evaporation. This was observable through lower brine conductivity at higher liquid flow rate for the same voltage. This is an expected result because higher flows produce bigger droplet diameters, longer break-up lengths and less spatial dispersion of the spray which eventually leads to shorter droplet residence time.

Following these experiments, a more systematic approach was taken using the four different liquid flow rates mentioned before and varying the electric potential from 0 kV to 4 kV in steps of 1 kV. In each configuration the evaporation was calculated using Eq. 2, the liquid inlet temperature was kept at ~ 80 °C and dry air at ambient temperature was injected in a counter flow (45 L min⁻¹) to keep relative humidity inside the reactor below saturation level. The results of these experiments are shown in Fig. 10.

In the plot, the *relative evaporation* (RE_{XkV}) shown for each data point is the ratio between the evaporation of the spray at a certain potential (E_{XkV}) and its value for the uncharged situation (E_{0kV}) expressed as a percentage as follows,

$$RE_{XkV} = \left(\frac{E_{XkV}}{E_{0kV}} - 1 \right) \cdot 100\% \quad (3)$$

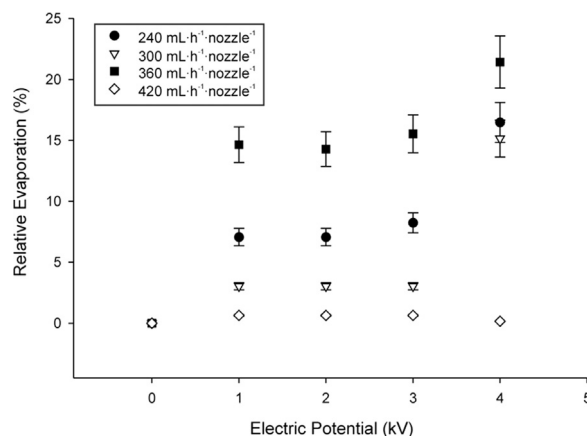


Fig. 10. Relative evaporation at different potentials (0–4 kV) for different liquid flow rates (240, 300, 360 and 420 mL h⁻¹·nozzle⁻¹). Spray temperature was ~80 °C, dry air at ambient temperature was injected in a counter flow at 45 L min⁻¹ and reactor internal temperature was 25 °C. Each data point represents the average of two measurements with the error bar representing the minimum and maximum measured values.

For the conditions of the experiments, the calculated evaporation of the uncharged sprays was always between 6% and 7% of the total atomized volume for all tested flows.

The plot shows that the application of the electric potential enhances the spray evaporation compared to the uncharged situation by up to 22% (8.5% of the total atomized volume). The best results were obtained with a liquid flow rate of 360 mL h⁻¹·nozzle⁻¹ and a potential difference of 4 kV. Previous experiments indicated that for this liquid flow rate the spray is already rather monodisperse even before the application of the electric field (Agostinho, Yurteri, Fuchs, Marijnissen et al., 2012), which could be a good indication of the role of the spray spatial dispersion and narrow size distribution in the evaporation process.

About the results obtained with 240 mL h⁻¹ nozzle⁻¹ the following can be said: At this flow level the evaporation calculated for the uncharged situation ($\Phi = 0$) was the lowest measured (5.8%). However, after the application of the electric potential, it increased to levels similar to those found for 300 and 360 mL h⁻¹·nozzle⁻¹ (~8.5%). Such (good) results are probably due to the fact that the influence of the electrical potential on reducing the droplet size for this liquid flow rate is much more pronounced than for the others, i.e. it can reduce the average primary droplet size up to 50% (Agostinho, Yurteri, Fuchs, Marijnissen et al., 2012). Additionally, it has been shown that the droplet spatial dispersion for this liquid flow rate is more pronounced at the same potential level than for the other investigated liquid flow rates because the break-up length is much shorter (Agostinho, Yurteri, Fuchs, & Tamminga, 2012).

For a liquid flow rate of 300 mL h⁻¹·nozzle⁻¹ the situation is very similar to the previous one, but the evaporation level for the initial potentials (1–3 kV) was lower. This can be explained because for these voltages the sprays produce droplets with similar diameter but the higher inertia of the droplets at 300 mL h⁻¹·nozzle⁻¹ decreases their spatial dispersion inside the chamber (Agostinho, Yurteri, Fuchs, & Tamminga, 2012).

The low values found for 420 mL h⁻¹·nozzle⁻¹ were probably a combined effect of the higher inertia of the droplets (shorter flying time) which also lead to less spatial dispersion and bigger droplets (Agostinho, Yurteri, Fuchs, & Tamminga, 2012).

It is important to mention that, during these experiments, the thermodynamic conditions were quite stable, i.e. reactor internal temperature, liquid inlet temperature and air flow rate were kept constant. This was also seen by the fact that the relative humidity level during the experiments was rather constant, i.e. between 85% and 90%.

The results are thus, a good indication that the manipulation of droplet size and spatial dispersion provided by EHDA strongly influences the evaporation process. To evaluate how strong this effect is compared to non EHDA related effects, further experiments were conducted varying the air flow rate and the liquid inlet temperature for the spray which presented the best performance. The results obtained are shown in Fig. 11.

Fig. 11a shows the influence of the injected dry air flow rate on the evaporation. It can be seen from the plot that, for a constant air flow, this influence increases with the electric potential. This can be related with the broader spatial dispersion of the spray at higher potentials which favors the removal of the produced vapor around the droplets liquid air interface. As indicated, for 75 L min⁻¹ and 4 kV the relative evaporation was ~40% higher than obtained for the uncharged situation (~10% of the total atomized volume). It was also observed that while the relative humidity inside the chamber for the highest air flow rates (75 and 85 L min⁻¹) was kept at ~16%, it reached up to 90% for the lowest values (35 and 45 L min⁻¹).

For the highest air flow (85 L min⁻¹) the relative evaporation was reduced when the potential reached 4 kV. A possible reason could be the blown out of small droplets via the chamber outlet. But such droplets were not detected using laser pointers. Other reasons could be the broaden up of the spray or deceleration of the droplets caused by the high air flow rate, i.e. which would increase the residence time. Such possibilities could not be carefully verified because the amount of vapor inside the chamber did not allow the visualization of the spray with the high speed system. However, the high differences seen between the evaporation level at low air flows (35 and 45 L min⁻¹) and high air flows (75 and 85 L min⁻¹) for the same potential, i.e. same droplet size and spatial dispersion, is a strong indication that the residence time of the droplets was higher for the high air flow experiments.

When applying the (dry air) flow rate which presented the best results (75 L min⁻¹) and varying spray initial temperatures (60

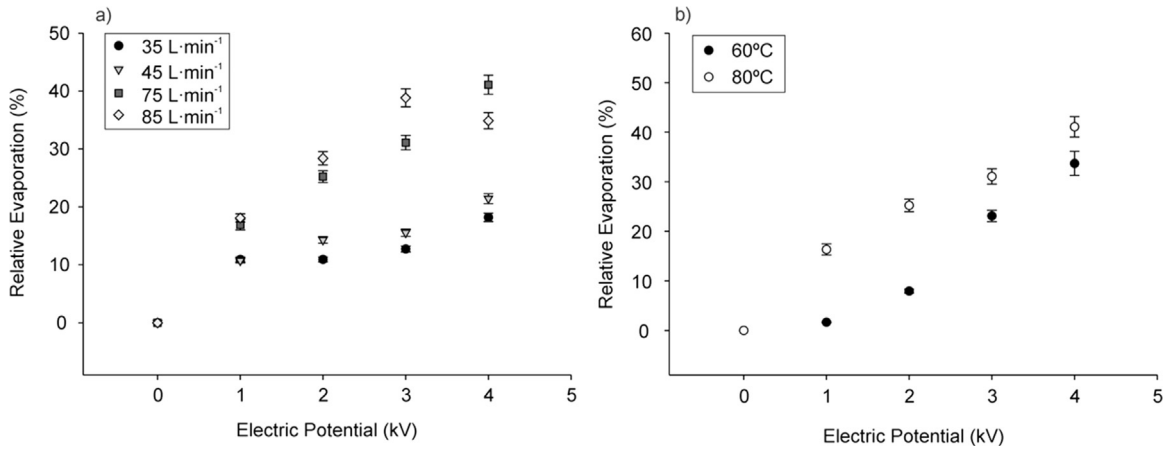


Fig. 11. Relative evaporation against electric potential for different flow rates of the injected dry air (a) and influence of the different spray initial temperature at a constant air flow rate of $75 \text{ L}\cdot\text{min}^{-1}$ (11b). Both experiments were done for $360 \text{ mL}\cdot\text{h}^{-1}\cdot\text{nozzle}^{-1}$ (best performance flow-rate found in the first experiments). Each data point represents the average of the two measurements with the error bar representing the minimum and maximum measured values.

and 80°C), as expected, we found higher temperatures to provide slightly better evaporation, i.e. $\sim 10\%$. However, this difference decreases significantly for higher potentials (4 kV) which is a good indication of the important role played by the spatial dispersion.

Finally, to have an idea about the energy performance of the proposed device, its droplet generation efficiency was calculated. For that, the theoretical energy required to generate droplets from a liquid, was estimated by calculating the necessary energy to create the surface of the droplets, i.e. the product of droplet surface area and surface tension (Eq. 4)(Liu, 1981).

$$E = \sigma\pi D^2 \quad (4)$$

where D is the average droplet diameter and σ is the surface tension of the liquid. In the above estimation the energy needed to overcome viscous forces during liquid break-up is neglected. Doing this for aqueous solutions as opposed to e.g. oils, is a valid assumption (Liu, 1981).

With high speed imaging we could estimate the number of droplets (N) generated in a certain time interval and measure their individual diameters. For each droplet the above mentioned equation was applied and the system “theoretical energy input” was calculated according to:

$$E_T = \sum_{i=1}^N E_i \quad (5)$$

Using the spray (average) electric current and the electric potential difference for the same time interval needed to produce the N droplets we calculated the electrical energy input of the system (E_E). From the pressure difference inside chamber A, and the liquid flow rate, we estimated the energy input for the pumping system for the same time interval (E_p). We then considered the atomizer “actual energy input” as:

$$E_A = E_E + E_p \quad (6)$$

Thus, the theoretical energy efficiency of our atomization method was calculated as:

$$\eta = \frac{E_T}{E_A} \quad (7)$$

In general this efficiency is very small because only a very small part of the input energy is converted into surface energy to generate the droplets. A large percentage is converted into kinetic energy and heat as reported by Liu (1981).

From the above mentioned values we determined that the theoretical energy efficiency of our system is, in average, $\sim 0.43\%$ while a typical efficiency for swirl atomizers running with water ($\Delta P = 10 \text{ MPa}$ driving force) is $\sim 0.22\%$ (Liu, 1981).

Regarding accumulation of (dry) salts on the nozzle surface, i.e. scaling, it could be observed that the nozzles remained operational after more than 72 h of continuous running. After long term experiments some salt crystals were observed at approximately 1 cm above the nozzle tip which were possibly formed due to evaporation of counter charged droplets attracted by the nozzle surface. This phenomenon has been previously mentioned by Agostinho *et al* for studies with the intermittent cone-jet mode (Agostinho, Fuchs, Metz, Yurteri, & Marijnissen, 2011).

Further studies with real sea water are needed to better quantify and understand scaling problems. Additionally, nozzle based systems naturally require good pre-treatment to remove suspended solids and avoid clogging. In this case, considering the nozzle inner diameter, microfiltration systems can be a good option. As scaling was only observed on the external part of the nozzle, other solutions would be, for example, a surface treatment of the nozzle outer walls with hydrophobic layers.

5. Conclusions

In this paper we present a short overview of electrospraying of water with a special emphasis on a high flow EHDA mode known as the simple-jet mode. Both experiments and the review presented in this aim at providing a better understanding of electrospray in the simple-jet as well as an insight about the influence that electrospray in this mode has on droplet (in air) evaporation.

Regarding the investigations done to further characterize and present electrospray in the simple-jet mode, the following can be mentioned: (i) the Weber number, i.e. commonly applied for the classification of droplet formation mechanisms in uncharged jets, is proposed as a non-dimensional constant to provide a more quantitative limit between the low flow EHDA modes, e.g. cone-jet mode, and the high flow EHDA mode, e.g. the simple-jet mode, (ii) regardless of the high liquid flow rate required to obtain the simple-jet mode, the applied electric field still exerts an important influence on both droplet size, size distribution and spatial dispersion (spray angle), (iii) for the varicose break-up, the influence of the electric potential on the primary droplet average size is higher if the droplet formation mechanism is in the transition regime ($We < 4$) than in the jetting regime ($We \geq 4$), (iv) in the whipping break-up, the electric potential can significantly decrease the average droplet size providing, in some cases, D_{80} smaller than the jet diameter.

Regarding the experiments conducted to evaluate the influence of electrospray in the simple-jet mode, with varicose break-up on droplet (in air) evaporation using a single step evaporation system, it can be inferred that droplet size, size distribution and spray angle play an important role on the evaporation efficiency of droplets in air. As presented, when adequately combined with other tools like forced convection and appropriate inlet temperature, the relative evaporation can be enhanced by up to 40%, compared to an uncharged situation.

Moreover, the easy manipulation of these parameters made possible by EHDA in the simple-jet mode is an important asset which should be utilized to further improve the understanding about their influence on the evaporation of the droplets in air.

Acknowledgements

The authors would like to thank the following institutes for valuable infra-structure and technical input during the realization of this work: Wetsus, European Centre of Excellence for Sustainable Water Technology and NHL University of Applied Sciences.

References

- A. M. Gañan-Calvo, J. D. A. A. B. (1997). Current and droplet size in the electrospraying of liquids. *Scaling Laws. Journal of Aerosol Science*, 28(2), 249–275.
- Agostinho, L. L. F. (2013). *Electrohydrodynamic atomization in the simple-jet mode. Out-scaling and application (PhD)*. Delft: TU Delft.
- Agostinho, L. L. F., Fuchs, E. C., Metz, S. J., Yurteri, C. U., & Marijnissen, J. C. M. (2011). Reverse movement and coalescence of water microdroplets in electrohydrodynamic atomization. *Physical Review E*, 84(2), 026317.
- Agostinho, L. L. F., Yurteri, C. U., Fuchs, E. C., & Marijnissen, J. C. M. (2012). Monodisperse water microdroplets generated by electrohydrodynamic atomization in the simple-jet mode. *Applied Physics Letters*, 100(24), 244105. <http://dx.doi.org/10.1063/1.4729021>.
- Agostinho, L. L. F., Yurteri, C. U., Fuchs, E. C., Tamminga, G., Brouwer, S. P., & Marijnissen, J. C. M. (2012). Morphology of water electrosprays in the simple-jet mode. *Physical Review E*, 86(6), 066317.
- Agostinho, L. L. F., Yurteri, C. U., Wartena, J., Brouwer, S. P., Fuchs, E. C., & Marijnissen, J. C. M. (2013). Insulated multinozzle system for electrohydrodynamic atomization in the simple-jet mode. *Applied Physics Letters*, 102(19), 194103. <http://dx.doi.org/10.1063/1.4806977>.
- Ambravaneswaran, B., Phillips, S. D., & Basaran, O. A. (2000). Theoretical analysis of a dripping faucet. *Physical Review Letters*, 85(25), 5332–5335.
- Ashgriz, N. (2011). *Hanbook of atomization and sprays. Hanbook of Atomization and Sprays*. Springer.
- Balachandran, W., Machowski, W., & Ahmad, C. N. (1992). 4-9 Oct. 1992). Electrostatic atomisation of conducting liquids using AC superimposed on DC fields. Paper presented at the Conference Record of the 1992 IEEE Industry Applications Society Annual Meeting.
- Boda, S. K., Li, X., & Xie, J. (2018). Electrospraying an enabling technology for pharmaceutical and biomedical applications: A review. *Journal of Aerosol Science*. <http://dx.doi.org/10.1016/j.jaerosci.2018.04.002> (Special edition EHDA).
- Borra, J.-P., Ehouarn, P., & Boulaud, D. (2004). Electrohydrodynamic atomisation of water stabilised by glow discharge – operating range and droplet properties. *Journal of Aerosol Science*, 35.
- Borra, J. P. (2018). Review on water electro-sprays and applications of charged droplets with focus on the corona-assisted cone jet mode for high efficiency particles air filtration by wet electro-scrubbing of aerosols. *Journal of Aerosol Science*. <http://dx.doi.org/10.1016/j.jaerosci.2018.04.005>.
- Borra, J. P., Camelot, D., Marijnissen, J. C. M., & Scarlett, B. (1997). A new production process of powders with defined properties by electrohydrodynamic atomization of liquids and post-production electrical mixing. *Journal of Electrostatics*, 40–41, 633–638. [http://dx.doi.org/10.1016/S0304-3886\(97\)00065-X](http://dx.doi.org/10.1016/S0304-3886(97)00065-X).
- Bos, B. (2017). Producing emulsions with electrohydrodynamic atomization (EHDA). Poster presented at the Wetsus Congress 2017, Synergy in Research and Innovation, Leeuwarden.
- Briceno-Gutierrez, D., Salinas-Barrera, V., Vargas-Hernández, Y., Gaete-Garretón, L., & Zanelli-Iglesias, C. (2015). On the ultrasonic atomization of liquids. *Physics Procedia*, 63, 37–41. <http://dx.doi.org/10.1016/j.phpro.2015.03.006>.
- Brouwer, S. P. (2011). *Design and characterization of a single-effect electrohydrodynamic desalinator. Mechanical Engineering, sustainable processes and energy technology (Master thesis)*. Leeuwarden: Delft University of Technology.
- Camelot, D., Marijnissen, J. C. M., & Scarlett, B. (1999). Bipolar coagulation process for the production of powders. *Industrial & Engineering Chemistry Research*, 38(3), 631–638. <http://dx.doi.org/10.1021/ie980435j>.
- Camelot, D. M. A., Brunner, D., Hartman, R. P. M., Marijnissen, J. C. M., & Scarlett, B. (1998). Mechanisms of jet break-up for EHDA in the cone-jet mode (doi: DOI: 10.1016/S0021-8502(98)90603-6) *Journal of Aerosol Science*, 29(Supplement 2), S841–S842.
- Castillo, J., Martin, S., Rodriguez-Perez, D., Higuera, F., & Garcia-Ybarra, P. (2018). Nanostructured porous coatings via electrospray atomization and deposition of nanoparticle suspensions. *Journal of Aerosol Science*. <http://dx.doi.org/10.1016/j.jaerosci.2018.03.004> (Special edition EHDA).
- Ciach, T. (2007). Application of electrohydrodynamic atomization in drug delivery. *Journal of Drug Delivery Science and Technology*, 17(6), 367–375. [http://dx.doi.org/10.1016/S1773-2247\(07\)50076-6](http://dx.doi.org/10.1016/S1773-2247(07)50076-6).
- Clanet, C., & Lasheras, J. C. (1999). Transition from dripping to jetting. *Journal of Fluid Mechanics*, 383, 307–326 (doi:null).
- Cloupeau, M., & Prunet-Foch, B. (1989). Electrostatic spraying of liquids in cone-jet mode (doi: DOI: 10.1016/0304-3886(89)90081-8) *Journal of Electrostatics*, 22(2), 135–159.
- Cloupeau, M., & Prunet-Foch, B. (1990). Electrostatic spraying of liquids: Main functioning modes. *Journal of Electrostatics*, 25(2), 165–184. [http://dx.doi.org/10.1016/0304-3886\(90\)90025-q](http://dx.doi.org/10.1016/0304-3886(90)90025-q).
- Cloupeau, M., & Prunet-Foch, B. (1994). Electrohydrodynamic spraying functioning modes: A critical review (doi: DOI: 10.1016/0021-8502(94)90199-6) *Journal of Aerosol Science*, 25(6), 1021–1036.

- Collins, R. T., Harris, M. T., & Basaran, O. A. (2007). Breakup of electrified jets. *Journal of Fluid Mechanics*, 588, 75–129. <http://dx.doi.org/10.1017/S0022112007007409>.
- Eggers, J., & Villermaux, E. (2008). Physics of liquid jets. *Reports on Progress in Physics*, 71(3), 036601.
- Gachara, C. W., Bos, B., Marijnissen, J., Gatari, M. J., & Agostinho, L. L. F. (2017). Electrohydrodynamic Atomization of a non-Newtonian solution with high solid content. Paper presented at the European Aerosol Conference 2017, Zurich.
- Gañan-Calvo, A. M., & Barrero, A. (1996). A global model for the electro-spraying of liquids in steady cone-jet mode. [doi: DOI: 10.1016/0021-8502(96)00162-0]. *Journal of Aerosol Science*, 27(Supplement 1), S179–S180.
- Gañan-Calvo, A. M., et al. (2009). Revision of capillary cone-jet physics: Electro-spray and flow focusing. *Physical Review E*, 79(6), 066305.
- Ganan-Calvo, A. M., Lopez-Herrera, J., Herrada, M., Ramos, A., & Montanero, J. M. (2018). Review on the physics of electro-spray: from electrokinetics to the operating conditions of Taylor cone-jets, and beyond. *Journal of Aerosol Science*. <http://dx.doi.org/10.1016/j.jaerosci.2018.05.002>.
- Geerse, K. B., & Marijnissen, J. C. M. (2003). *Electrospray as means to produce monodisperse drug particles*. Dordrecht: Springer.
- Geerse, K. B., Marijnissen, J. C. M., Kerssies, A., van der Staaij, M., & Scarlett, B. (1999). The application of electrohydrodynamic atomization in greenhouses (doi: DOI: 10.1016/S0021-8502(99)(80288-2) *Journal of Aerosol Science*, 30(Supplement 1), S553–S554.
- Grace, J. M., & Marijnissen, J. C. M. (1994). A review of liquid atomization by electrical means (doi: DOI: 10.1016/0021-8502(94)(90198-8) *Journal of Aerosol Science*, 25(6), 1005–1019.
- Hartman, R. P. A., Brunner, D. J., Camelot, D. M. A., Marijnissen, J. C. M., & Scarlett, B. (1999). Electrohydrodynamic atomization in the cone-jet mode. physical modeling of the liquid cone and jet (doi: DOI: 10.1016/S0021-8502(99)(00033-6) *Journal of Aerosol Science*, 30(7), 823–849.
- Hartman, R. P. A., Brunner, D. J., Camelot, D. M. A., Marijnissen, J. C. M., & Scarlett, B. (2000). Jet break-up in electrohydrodynamic atomization in the cone-jet mode (doi: DOI: 10.1016/S0021-8502(99)(00034-8) *Journal of Aerosol Science*, 31(1), 65–95.
- Hartman, R. P. A., Marijnissen, J. C. M., & Scarlett, B. (1997). Electro hydrodynamic atomization in the cone-jet mode. A physical model of the liquid cone and jet (doi: DOI: 10.1016/S0021-8502(97)(85263-9) *Journal of Aerosol Science*, 28(Supplement 1), S527–S528.
- Hoeve, W. V., Gekle, S., Snoeijer, J. H., Versluis, M., Brenner, M. P., & Lohse, D. (2010). Breakup of diminutive Rayleigh jets. *Physics of Fluids*, 22(12), 122003.
- Hohman, M. M., Shin, M., Rutledge, G., & Brenner, M. P. (2001aa). Electrospinning and electrically forced jets. I. Stability theory. *Physics of Fluids*, 13(8), 2201–2220.
- Hohman, M. M., Shin, M., Rutledge, G., & Brenner, M. P. (2001bb). Electrospinning and electrically forced jets. II. *Applications Physics of Fluids*, 13(8), 2221–2236.
- Jaworek, A., Krupa, A., & Sobczyk, A. T. (2018). Electro-spray application to powder production and surface coating. *Journal of Aerosol Science*. <http://dx.doi.org/10.1016/j.jaerosci.2018.04.006> (Special edition EHDA).
- Jaworek, A., Sobczyk, A. T., Krupa, A., Marchewicz, A., Krella, A., & Czech, T. (2016). *Thin films by EHDA - A review* (Vol. 10).
- Juraschek, R., & Röllgen, F. W. (1998). Pulsation phenomena during electro-spray ionization (doi: 10.1016/S1387-3806(98)(14025-3) *International Journal of Mass Spectrometry*, 177(1), 1–15.
- Kamau, A. B. B., Agostinho, L. L. F., Gatari, M. J., Marijnissen, J. (2017). Analysis of different liquid-liquid combinations and conditions for the formation of a stable cone-jet mode in electro-spray emulsification processes. Paper presented at the European Aerosol Conference, Zurich.
- Kelder, E., Marijnissen, J. C. M., & Waiyego, S. K. (2018). EDHA for energy production, storage and conversion devices. *Journal of Aerosol Science*. <http://dx.doi.org/10.1016/j.jaerosci.2018.04.011> (Special edition EHDA).
- Lafrance, P. (1975). Nonlinear breakup of a laminar liquid jet. *Physics of Fluids*, 18(4), 428–432.
- Li, T., Nishida, K., & Hiroyasu, H. (2011). Droplet size distribution and evaporation characteristics of fuel spray by a swirl type atomizer. *Fuel*, 90(7), 2367–2376. <http://dx.doi.org/10.1016/j.fuel.2011.03.011>.
- Liu, C., Liu, F., Yang, J., Mu, Y., Hu, C., & Xu, G. (2018). Experimental investigations of spray generated by a pressure swirl atomizer. *Journal of the Energy Institute*. <http://dx.doi.org/10.1016/j.joei.2018.01.014>.
- Liu, H. (1981). *Science and engineering of droplets*. 01. New York: William Andrew.
- Loscertales, I. G., Barrero, A., Guerrero, I., Cortijo, R., Marquez, M., & Ganan-Calvo, A. M. (2002). Micro/nano encapsulation via electrified coaxial liquid jets. *Science*, 295(5560), 1695–1698.
- Nguyen, D. N., Clasen, C., & Van den Mooter, G. (2016). Pharmaceutical applications of electro-spraying. *Journal of Pharmaceutical Sciences*, 105(9), 2601–2620. <http://dx.doi.org/10.1016/j.xphs.2016.04.024>.
- Ondimu, O., Marijnissen, J., Agostinho, L. L. F., Ganesan, V., & Gatari, M. J. (2017). Modeling simple-jet mode electrohydrodynamic-atomization droplets' trajectories and spray pattern for a single nozzle system. *Journal of Electrostatics*.
- Ondimu, O. M., Ganesan, V. A., Gatari, M. J., Marijnissen, J. C. M., & Agostinho, L. L. F. (2017). Modeling simple-jet mode electrohydrodynamic-atomization droplets' trajectories and spray pattern for a single nozzle system. *Journal of Electrostatics*, 89(Supplement C), 77–87. <http://dx.doi.org/10.1016/j.elstat.2017.08.001>.
- P. Maniarsan, J. R. P., & Nicholas, M. T. (2009). Design and performance evaluation of swirl injectors for water evaporation at low pressure. *Desalination*, 235, 139–145. <http://dx.doi.org/10.1016/j.desal.2008.02.007>.
- Park, I., Hong, W. S., Kim, S. B., & Kim, S. S. (2017). Experimental investigations on characteristics of stable water electro-spray in air without discharge. *Physical Review E*, 95(6), 063110.
- Parmentier, D., Rybałowska, A., van Smeden, J., Kroon, M. C., Marijnissen, J. C. M., & Agostinho, L. L. F. (2016). Applying electrohydrodynamic atomization to enhance mass transfer of metal salts from an aqueous phase towards ionic liquids. *Journal of Electrostatics*, 80, 1–7. <http://dx.doi.org/10.1016/j.elstat.2015.11.007>.
- Rayleigh, L. (1879). On the stability of jets. *Proceedings of the London Mathematical Society*, 10.
- Rosell-Llompart, J., Grifoll, J., & Loscertales, I. G. (2018). Electro-sprays in the cone-jet mode: from Taylor cone formation to spray development. *Journal of Aerosol Science*. <http://dx.doi.org/10.1016/j.jaerosci.2018.04.008>.
- Sinha, A., Surya Prakash, R., Madan Mohan, A., & Ravikrishna, R. V. (2016). Experimental studies on evaporation of fuel droplets under forced convection using spray in crossflow methodology. *Fuel*, 164(Supplement C), 374–385. <http://dx.doi.org/10.1016/j.fuel.2015.09.088>.
- Siringano, W. A. (2010). *Fluid dynamics and transport of droplets and sprays* (2nd ed.). Cambridge University Press.
- Stachewicz, U., Dijkman, J. F., Burdinski, D., Yurteri, C. U., & Marijnissen, J. C. M. (2009). Relaxation times in single event electro-spraying controlled by nozzle front surface modification (doi: 10.1021/la8021408) *Langmuir*, 25(4), 2540–2549. <http://dx.doi.org/10.1021/la8021408>.
- Tang, K., & Gomez, A. (1995). Generation of monodisperse water droplets from electro-sprays in a corona-assisted cone-jet mode (doi: DOI: 10.1006/jcis.1995.1464) *Journal of Colloid and Interface Science*, 175(2), 326–332.
- Tang, K., Page, J. S., Kelly, R. T., & Marginean, I. (2017). Electro-spray ionization in mass spectrometry A2 - Lindon, John C. In G. E. Tranter, & D. W. Koppenaal (Eds.). *Encyclopedia of spectroscopy and spectrometry* (pp. 476–481). (Third ed.). Oxford: Academic Press.
- Taylor, G. (1969). Electrically driven jets. *Proceedings of the Royal Society of London A Mathematical and Physical Sciences*, 313(1515), 453–475. <http://dx.doi.org/10.1098/rspa.1969.0205>.
- Wang, C., Xu, R., Song, Y., & Jiang, P. (2017). Study on water droplet flash evaporation in vacuum spray cooling. *International Journal of Heat and Mass Transfer*, 112(Supplement C), 279–288. <http://dx.doi.org/10.1016/j.ijheatmasstransfer.2017.04.111>.
- Williams, F. A. (1958). Spray combustion and atomization. *The Physics of Fluids*, 1(6), 541–545.
- Zeleny, J. (1917). Instability of electrified liquid surfaces. *Physical Review*, 10(1), 1.